Effect of Neutron Irradiation on the Ductility of 316 Stainless Steel

R. Lott

April 1973

UWFDM-61

FUSION TECHNOLOGY INSTITUTE

UNIVERSITY OF WISCONSIN

MADISON WISCONSIN

Effect of Neutron Irradiation on the Ductility of 316 Stainless Steel

R. Lott

Fusion Technology Institute
University of Wisconsin
1500 Engineering Drive
Madison, WI 53706

http://fti.neep.wisc.edu

April 1973

UWFDM-61

EFFECT OF NEUTRON IRRADIATION ON THE DUCTILITY OF 316 STAINLESS STEEL

by

Randy Lott

April 1973

FDM 61

University of Wisconsin

Ductility is generally defined as the ability of a material to deform plastically without fracturing. Materials that are easily deformed are termed ductile in contrast to brittle materials, which will fracture before their shape can be changed. Ductility, however, is a difficult parameter to define quantitatively. There are many methods for measuring the ductility of a material and each method may give a different result. All of these measurements are very sensitive to specimen geometry and testing conditions. The designer can seldom use ductility to predict how a particular section of material will behave in service. When ductility measurements are to be used for design purposes, it is important to choose measurements that are relevant to the application.

High ductility, coupled with high strength, is important to structures which must withstand high loads. Materials that can undergo large deformation when subjected to large forces are capable of absorbing great amounts of energy. The ability to absorb energy is particularly important when considering accident situations. Ductile materials may also deform to relieve high stress gradients and prevent premature failure in specimens where notches and inclusions cause stress concentrations. Materials which must be worked into components for any system must also be ductile.

Irradiation can have serious effects on the ductility of many of the structural components of any nuclear system. Fuel cladding in both thermal and fast fission reactors may become extremely brittle as they are subjected to high neutron fluences. The change in ductile to brittle

transition temperature of the ferritic steels used in reactor pressure vessels has also been an area of major concern. In fusion reactors, where the structural materials will be subjected to high fluences of high energy neutrons, embrittlement will be severe. Irradiation embrittlement is caused by two closely coupled phenomena - gas production and displacement damage. Helium and hydrogen are produced in the structural material through transmutations.[1] The formation of gas bubbles can lead to loss in ductility. Displacement damage can lead to the formation of loops and voids, which may also embrittle the material.

Tensile Test[2,3]

The tensile test is the most common method of measuring ductility. In the tensile test, a aniaxial load is applied to a standard tensile specimen, and the percent elongation of the specimen is measured as a function of the stress in the specimen. The results of this test are sensitive to specimen shape size and loading as well as the strain rate.[20,21] In the United States, there are standard specimens with both circular and square cross sections. The standard round bar specimen has a length of 2.0 inches and a diameter of .505 inches.

The results of a tensile test can be displayed on a true stress-true strain curve, as shown in Figure I. The true stress, σ_t, is taken to be the load applied divided by the maximum cross sectional area at each instant of time. The true strain, ε, is defined by the relation

$$\varepsilon = \int_{l_o}^{l} \frac{dl}{l}$$

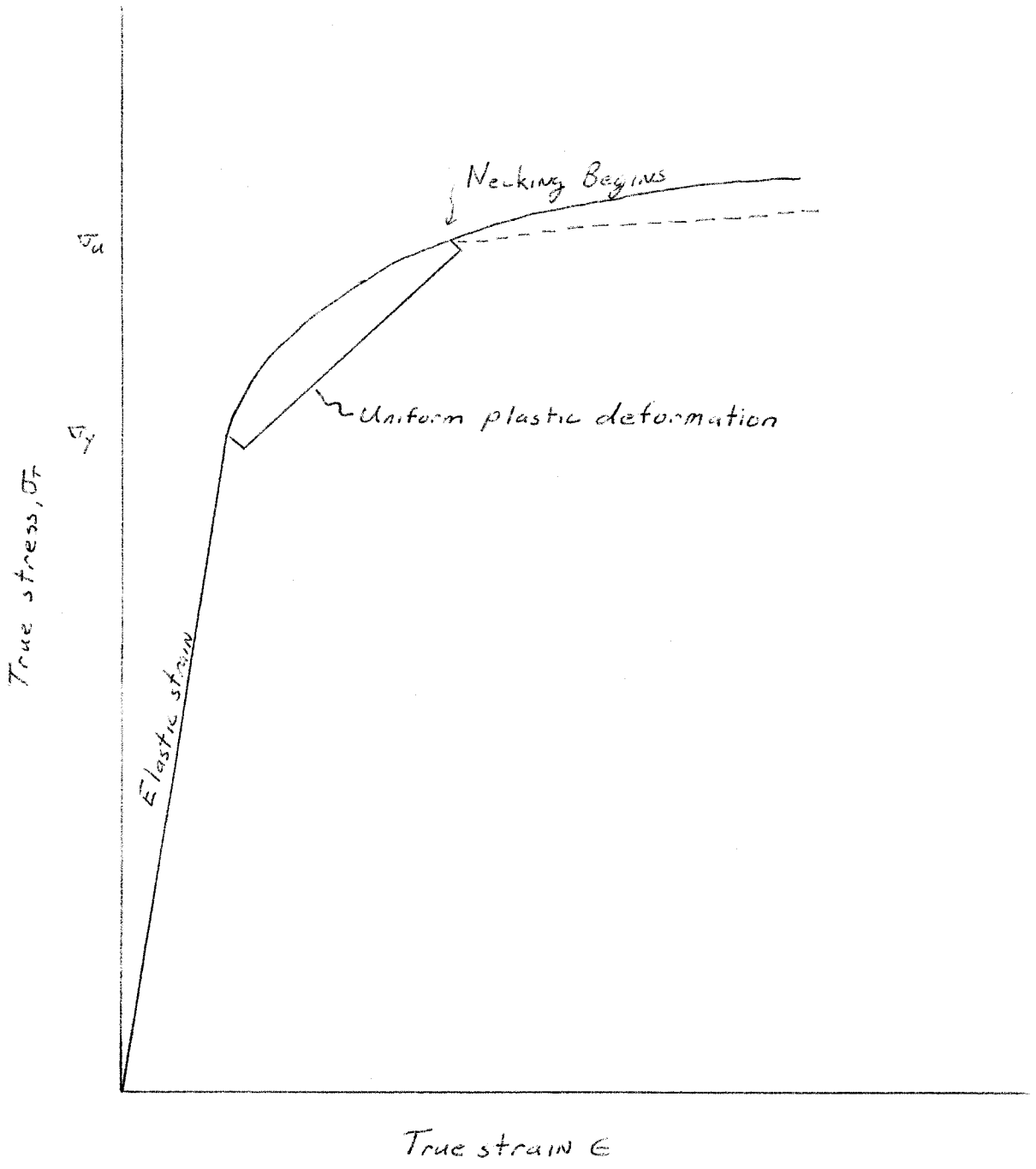
Necking Begins
σ_u
σ_y
Uniform plastic deformation
Elastic strain
True stress, σ_T
True strain ϵ

Figure I

where l is the specimen length and lo is the unstrained specimen length. If the specimen has undergone a total change in length Δl, the true strain may be evaluated from the integral;

$$\varepsilon = \ln \left(\frac{lo + \Delta l}{lo}\right)$$

The true stress-true strain curve can be divided into three regions. The first region is the elastic region, where the stress and strain are related linearly. All of the strain undergone in the elastic region can be recovered upon relaxation of the stress. The stress at which the elastic behavior terminates is called the yield stress. In the second region, the specimen undergoes uniform plastic elongation. The strain in this region occurs uniformly along the length of the specimen and is not recoverable. The empirical relation between true stress and true strain is

$$\sigma_t = K\varepsilon^n$$

In this relation, both K and n are constants. The constant n is the strain hardening exponent and is a measure of the increasing resistance to strain with higher strain. The region of uniform plastic deformation ends at the point where true strain is equal to the strain hardening exponent. In this region, the deformation results from necking of the specimen. As the specimen necks, the deformation occurs in a limited portion of the specimen. A triaxial stress distribution is set up as the specimen necks, which complicates the analysis. The dotted line in Figure I represents a correction of data to include only the uniaxial portion of the stress. The more common method of

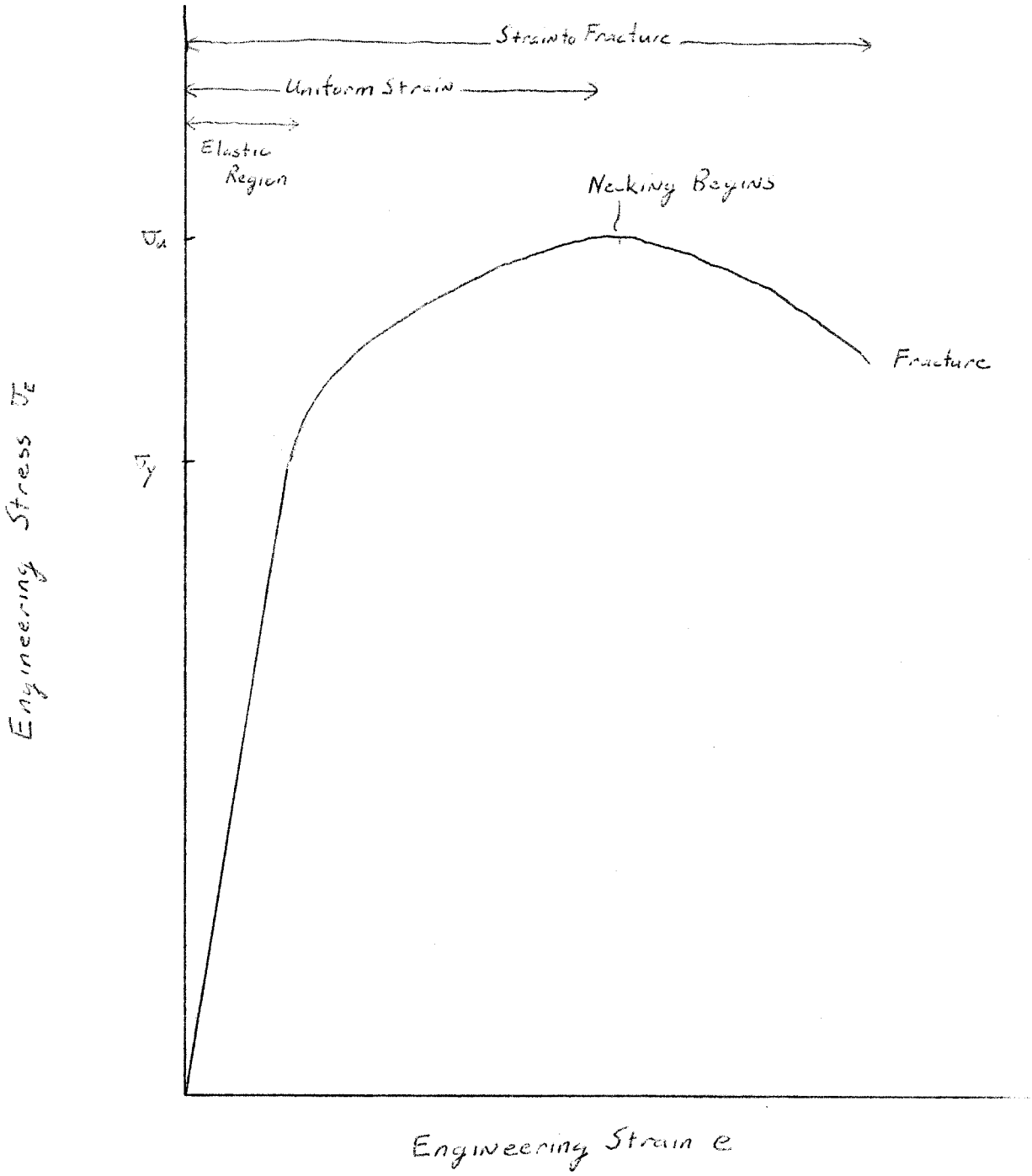
Strain to Fracture
Uniform Strain
Elastic Region
Necking Begins
σ_u
σ_y
Fracture
Engineering Stress σ_E
Engineering Strain e

Figure II

representing the results of a tensile test is the engineering stress-strain curve. The engineering stress, σ_e, is the load applied to the specimen divided by the original cross-sectional area. The engineering strain, e, is defined as the change in the total length, Δl, divided by the original length lo. The relation between true strain and engineering strain is

$$\varepsilon = \ln (1 + e)$$

The regions that were indentified on Figure I can also be seen in the typical engineering stress-strain curve shown in Figure II. The elastic portion of the curve is essentially the same for both curves. The engineering yield strength is not significantly different from the true yield stress. The maximum in the engineering stress is called the ultimate stress, σu, and occurs at the onset of necking. As necking occurs, the cross sectional area is reduced much faster than the true stress is increased, so the engineering stress falls off.

There are several measurements of ductility that can be made in a tensile test. The strain referred to in all of these measurements is the engineering strain. Total elongation is the value of the engineering strain at fracture. Uniform elongation is the value of the engineering strain when the ultimate stress is reached. In applications where necking is not acceptable, uniform elongation is used as a measure of ductility. As shown in Figure II, total and uniform elongation may be read directly from the engineering stress-strain curve. A third important measurement of ductility is reduction

in area: the ratio of cross sectional area at fracture to the original cross sectional area. Reduction in area is an indication of the importance of necking in the fracture of the specimen.

Although the tensile test was designed to be as simple as possible, a thorough analysis of the test is hopelessly complex. Specimen size as well as shape may determine the actual tensile behavior of the specimen. Necking is a highly localized phenomena and the total elongation measured in a sample will be a strong function of gage length. To avoid this problem, the zero-gage-length elongation, e_o, is computed assuming a constancy of volume. If the original cross-sectional area is A_o and the cross-sectional area at fracture is A, the zero length elongation can be computed from the relation

$$e_o = \frac{A_o}{A} - 1$$

Unfortunately, there are very few applications for which tensile test results are relevant. Generally, each component is subjected to a complex, triaxial stress.

Fracture of Unirradiated Stainless Steel

Before one can understand the ductility of any material, it is important to know how it fails. The failure mode of unirradiated stainless steel depends upon the test temperature. The temperature range can be divided into three regions,[4] low, intermediate and high.

In the low temperature region, (<650°C), fracture occurs by the

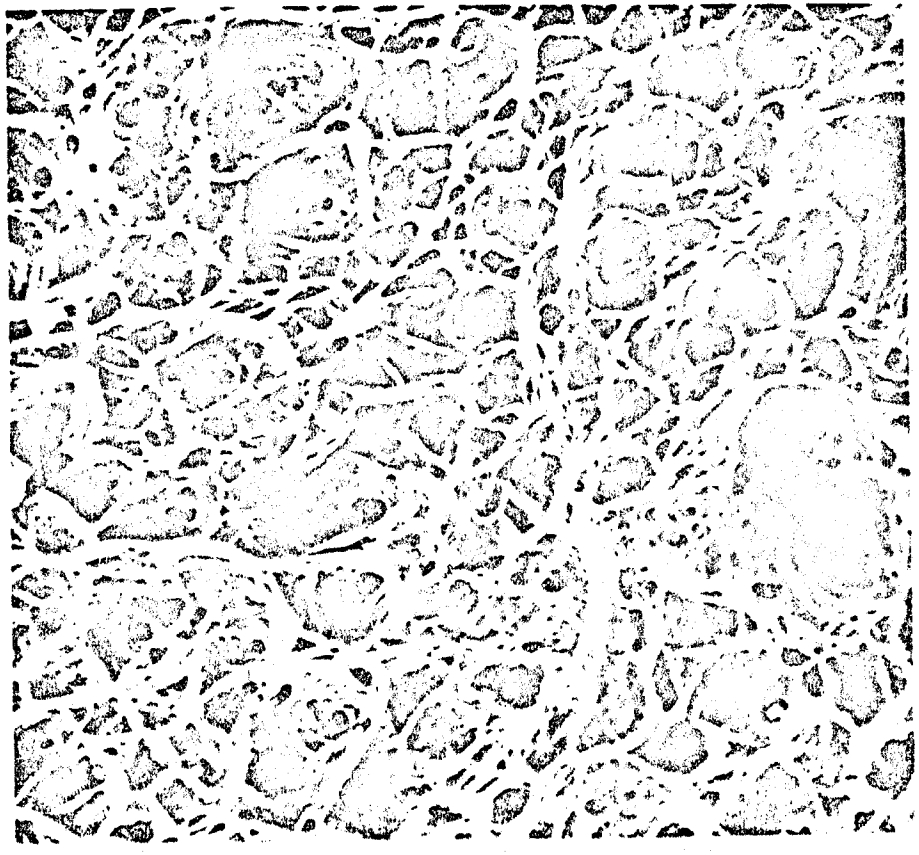

FIGURE III - REFERENCE 24 1000X

Scanning Electron Microscope Fractograph Showing the Typical Transgranular Plastic Dimpling Fracture of Unirradiated Stainless Steel

formation of voids within the grains. This intragranular type of fracture takes place as the voids grow through the plastic deformation of the surrounding material. The internal voids are nucleated when dislocations begin to pile-up on inclusions or precipitates within the grain. Figure III shows a scanning electron microscope fractograph of a tensile specimen that has failed by the formation of internal voids. Characteristically, the fracture surface of this specimen exhibits shear rupture dimples, which are the result of the growth of internal voids.

In the high temperature (>760°C), fracture occurs as a result of grain boundary sliding. Voids which form on the grain boundaries are responsible for this intergranular mode of fracture. As the surrounding material slides, any obstacle to grain boundary sliding may serve as a formation site for a void. The most common grain boundary obstacles are triple points, boundary irregularities and inclusions on the boundary. With continued stress, these voids will grow and eventually coalesce, forming internal cracks, which lead to failure. A micrograph of a stainless steel tensile specimen that has failed by intergranular fracture is shown in Figure IV. In this type of fracture, the grains appear to be pulled apart. Transition to intergranular fracture usually results in very little necking and reduced total elongation.

In the intermediate temperature range (650-760°C), a transition between intragranular and intergranular failure occurs. Above 650°C, the ductility begins to decline as the intergranular mode becomes increasingly important.

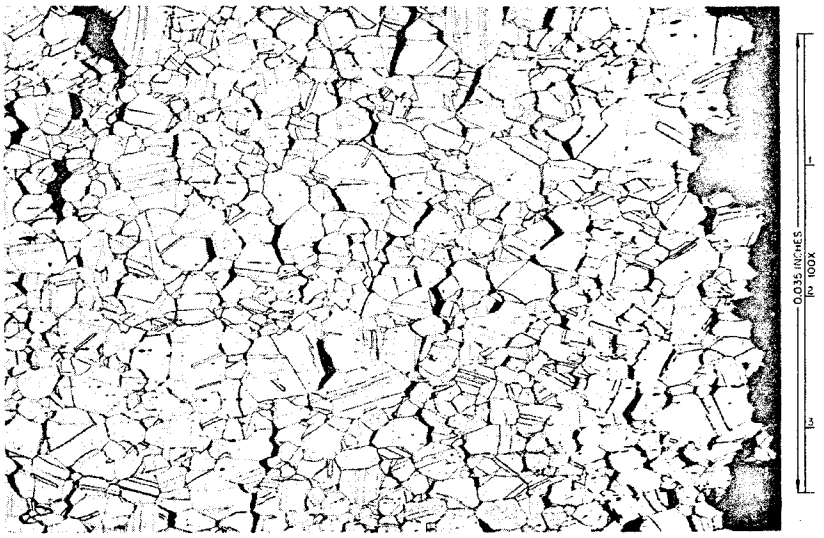

[redacted]. *Characteristics of high-temperature fracture in type 304 stainless steel. Stress was applied in the horizontal direction. Note the high density of intergranular cracks with the characteristic wedge appearance located below the fracture surface.*

FIGURE IV - REFERENCE 2

Irradiation Effects on Failure Mechanisms

The ductility of irradiated materials is reduced by two mechanisms, displacement damage and gas production. Point defects produced in the material during irradiation may precipitate into voids and dislocations.[5] These defects than act as barriers to dislocation movement, strengthening the matrix while at the same time reducing its ability to deform. Gas production during irradiation has been discussed by the author previously.[1] Both helium and hydrogen may have detrimental effects on ductility, but helium is generally felt to be the most harmful. Hydrogen embrittlement in prospective fusion reactor materials has been discussed elsewhere,[6] and will not be considered here. The formation of helium bubbles on grain boundaries promotes intergranular fracture. Although these two embrittlement mechanisms are inter-related to some unknown extent, they will initially be considered separately.

Displacement Damage

The formation of voids and dislocation loops in irradiated stainless steel are responsible for matrix hardening. At high temperatures, all of the defects (except gas bubbles) anneal out and matrix hardening will not occur. The inability of dislocations to pass through the matrix and pile up on isolated defects prevents the formation of internal voids large enough to cause failure. However, a new type of intragranular fracture has been noted in materials tested at temperatures where intergranular fracture is not predominant.[7,24] Figure V shows the fracture surfaces of three different tensile specimens of

FIGURE V - REFERENCE 7

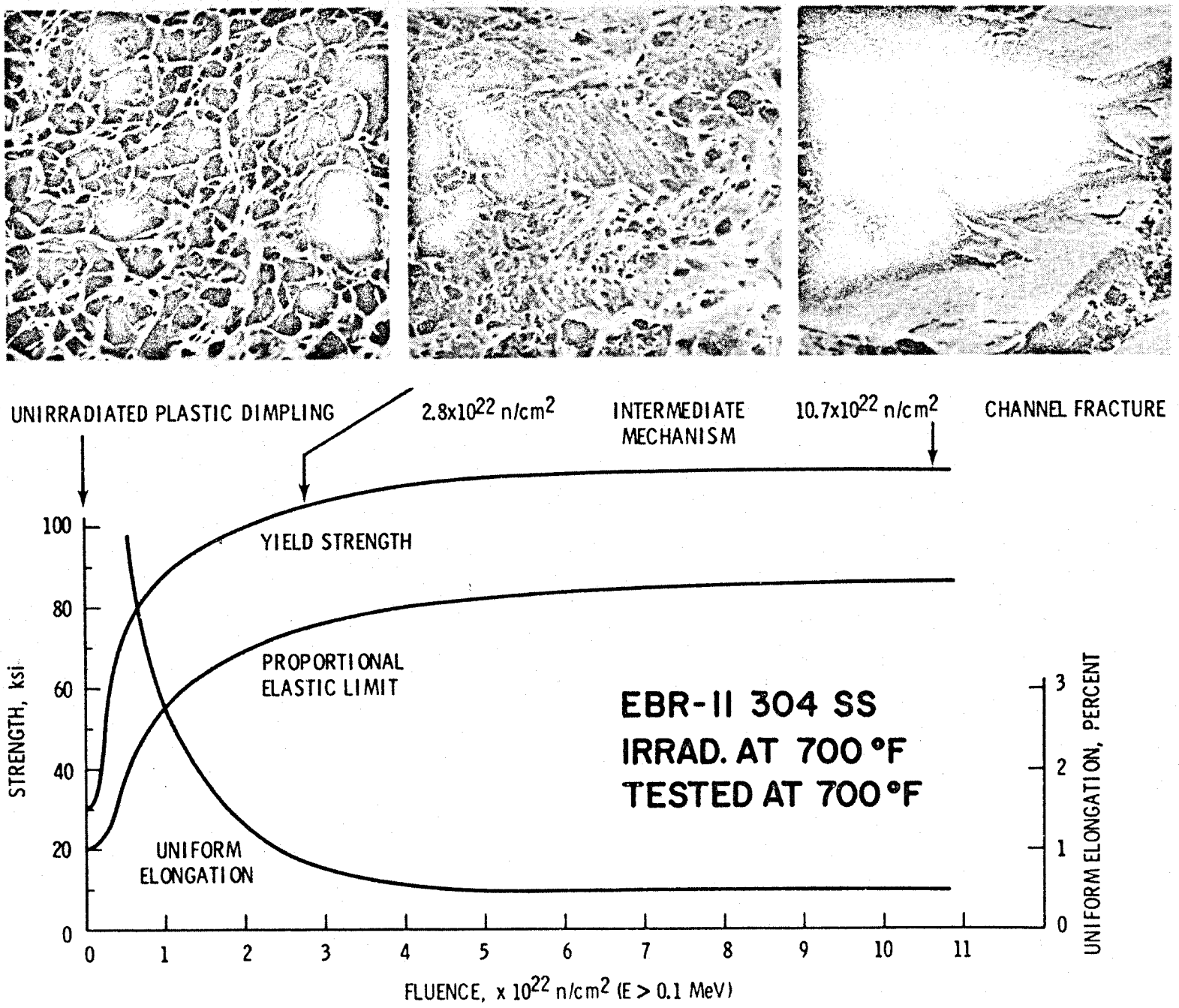

304 stainless steel irradiated in EBR-II at a temperature of 370°C and tested at the same temperature. The unirradiated specimen exhibits sheer rupture dimples, while the high fluence specimen has a smooth fracture surface; and the specimen irradiated to an intermediate flux level shows a transition between the two mechanisms. This second mode of fracture which is referred to as channel fracture is caused by the concentration of slip in narrow bands within the grain. If a single dislocation can be pushed through a strain hardened matrix, it may clear a path with other defects may follow. The concentration of all of the dislocation movement to a single plane causes the crystal to literally slip apart.

In higher temperature regions, matrix hardening can promote intergranular fracture. By hardening the matrix, irradiation can concentrate stress on the grain boundaries which will result in increased grain boundary sliding.

Helium Embrittlement

Studies of helium embrittlement in stainless steel fall into two categories - those which use neutron irradiated specimens[8,9,10,11] and those which use specimens injected with high energy helium ions.[4,25,26,27] Neutron irradiated samples usually come from large irradiation facilities such as EBR-II. A large amount of displacement damage is produced along with the helium. In order to study the effect of helium embrittlement alone, this displacement damage must be annealed out of the specimen. Unfortunately, this annealling process precludes any low temperature studies of helium embrittlement. High energy helium ions have been injected into specimens to obtain helium concentrations up to 40 appm,[25] with relatively low amounts of displacement damage. However, this

injection method must be limited to extremely thin specimens.

Another method for doping samples with helium has been proposed, but never used. Large tensile specimens could be doped with tritium, which has areasonable solubility in stainless steel. The tritium could then be frozen into the matrix and allowed to decay to helium-3. When the desired amount of helium has been produced, the tritium could be allowed to diffuse back out of the specimen leaving a large tensile specimen containing helium with no displacement damage.

Because it is highly insoluble in the metal matrix, helium will form gas bubbles in stainless steel. A threshold temperature for the formation of bubbles has been observed around 540°C. The size of these helium bubbles increases with temperature. Bubbles are usually associated with precipitates, dislocations and grain boundaries. It is not known if the bubbles nucleate homogeneously and migrate to these sites while they are still too small to be observed. In specimens irradiated in thermal fluxes, helium bubbles have been associated with boron containing precipitates.[10,11] However, in fast reactors and fusion reactors, the metal atoms will produce the major portion of the helium and this effect should not be so pronounced.

The helium bubbles that form on the grain boundaries enhance intergranular fracture. Gas bubbles become trapped on grain boundary precipitates (usually carbides) and triple points. These bubbles provide nuclei for the grain boundary cracks that lead to intergranular failure. The work of Kramer et. al.[4] on the effect of helium content on the total elongation of annealed type 304 stainless steel as a

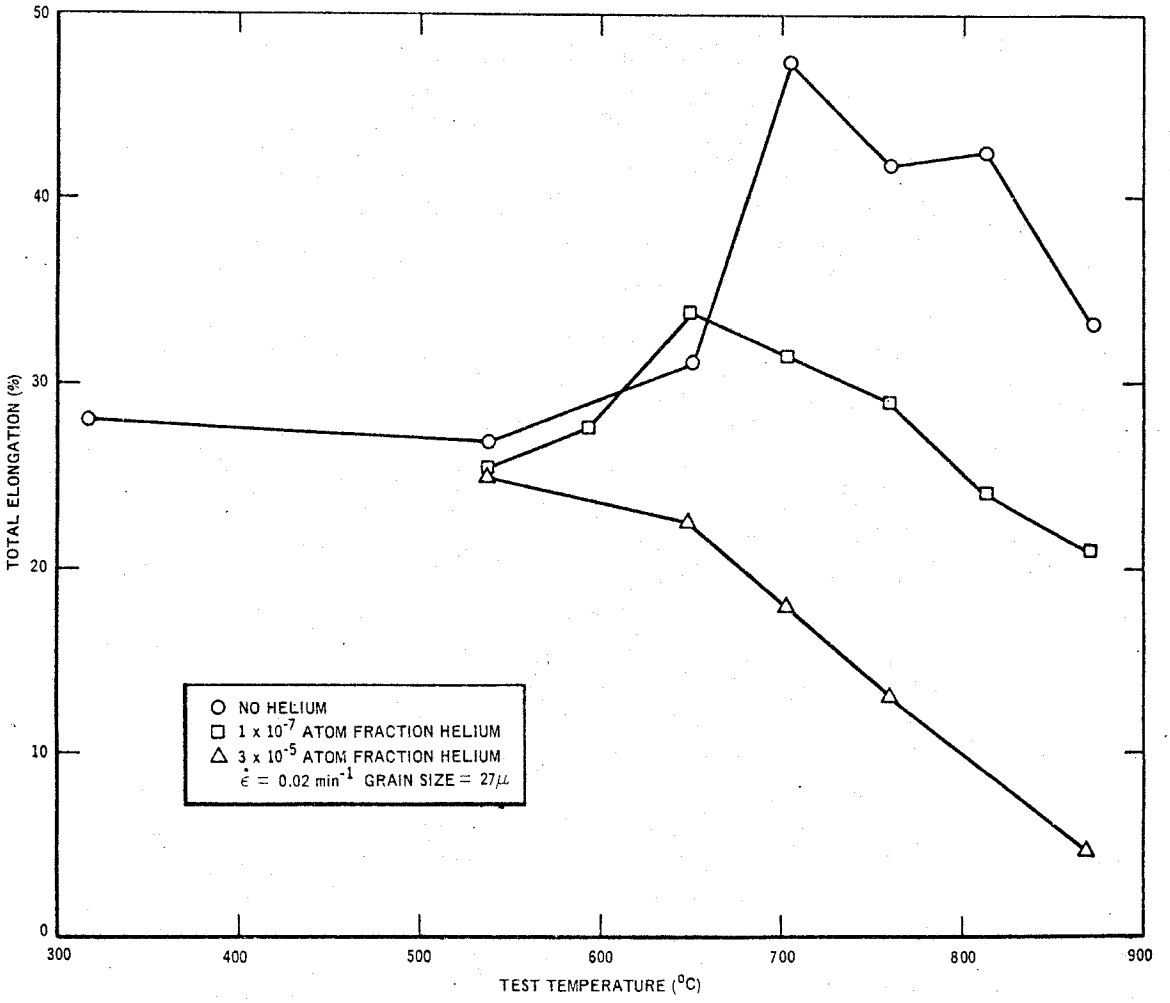

Total elongation vs test temperature for type 304 stainless steel with and without helium. Samples were annealed 10 h at 760 °C prior to testing.

FIGURE VI - REFERENCE 4

function of test temperature is presented in Figure VI. Below 540°C, the failure is intragranular and the helium content has little effect. At 540°C, the sample containing 30 atomic parts per million helium begins to show severe embrittlement when compared to the control sample. The sample containing 0.1 atomic parts per million of helium exhibits an intermediate behavior. The ductility of this low-helium sample does not begin to fall off until a test temperature of 650°C is reached and the degree of embrittlement, while severe, is not as severe as the sample containing a high concentration of helium.

Kangilaski et. al.[8] have performed tests on neutron irradiated specimens which have been annealed at 980°C to remove the displacement damage. When these specimens were tested at 500°C, they showed tensile properties similar to those of the unirradiated control. However, transmission electron microscope studies of these specimens showed that they contained a large number of 200-500Å diameter helium bubbles. These bubbles were formed during the annealing process. From these results, the authors argue that the large bubbles are not solely responsible for helium embrittlement. They claim that small, unobservable bubbles are responsible for most of the embrittlement. However, if the fracture mode at this temperature is still intragranular, the presence of bubbles on the grain boundary would have little effect.

Embrittlement in Neutron Irradiation

Matrix hardening and gas bubbles may act synergistically to reduce ductility.[12] At temperatures above the bubble formation threshold and below the recrystallization temperature, both helium embrittlement

Effect of Temperature on the Ductility of Irradiated 316 SS

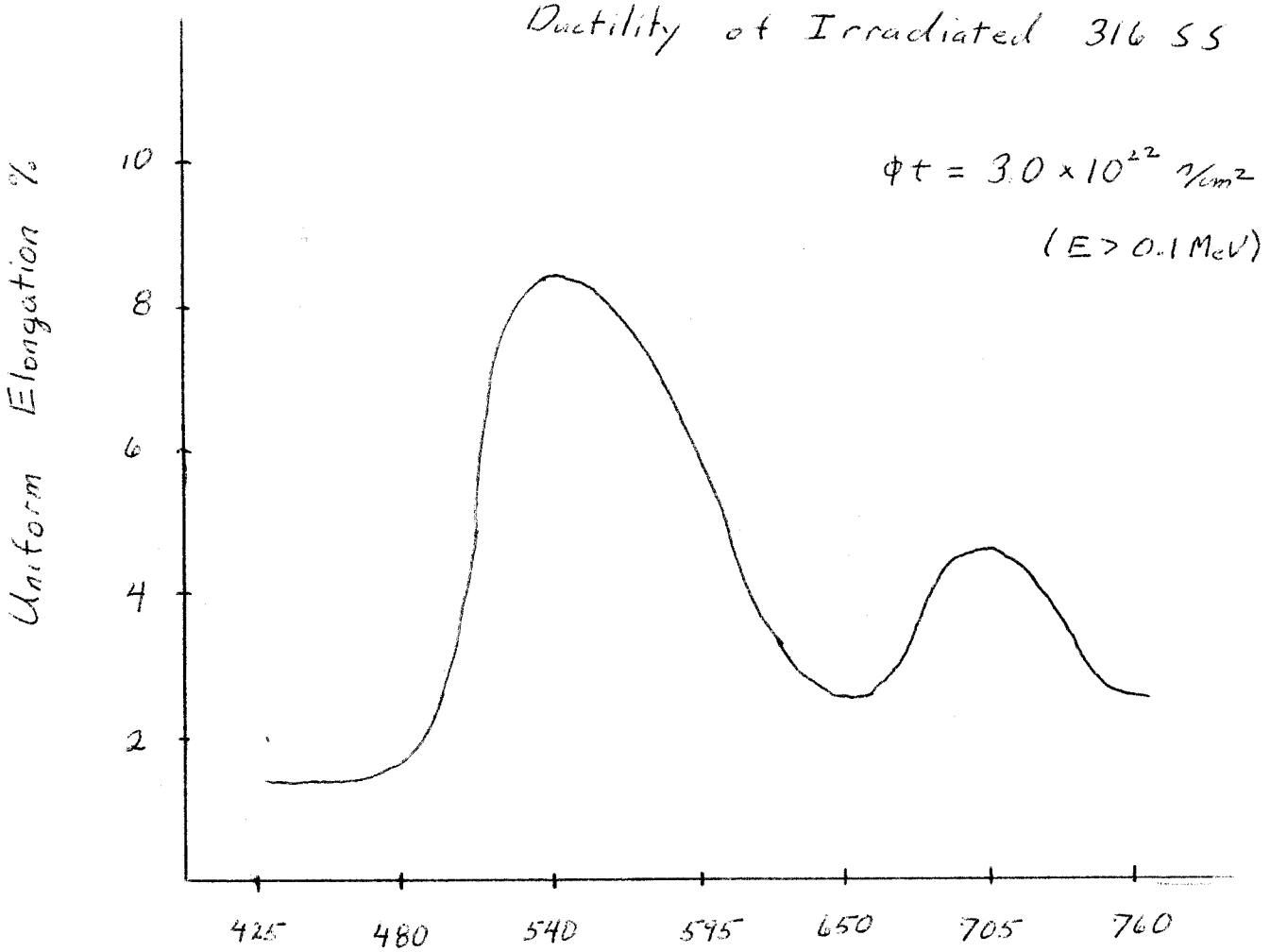

samples irradiated and tested at same temp

Figure VII

Ref 13.
R.L. Fish and J.J. Holmes, HEDL-SA-421

and matrix hardening will occur simultaneously. Because no slip takes place within the grains, stresses on the grain boundaries that might normally be relieved by deformation within the grain may result in grain boundary slippage. In this intermediate temperature range, the decrease in ductility is much larger than might be predicted by considereing helium embrittlement and matrix hardening separately. The range and effect of each ductility loss mechanism can be seen in Figure VII. Here uniform elongation is plotted as a function of temperature. These results were compiled by Fish and Holmes[13] from annealed 316 stainless steel irradiated in EBR-II. All of the specimens examined were irradiated to a constant fluence of 3.0×10^{22} nvt ($E > 0.1$ MeV). In all cases, the irradiation temperature was the same as the test temperature. At low temperatures (<480°C) the failure mode is primarily intragranular and the large density of small defects hardens the matrix. As the temperature is increased (480-540°C) the defects become larger, but their density is decreased. As the defect concentration becomes lower, the matrix becomes more deformable and there is an increase in ductility. Around 540°C, helium bubbles begin to form. In the region between 540°C and 650°C, the helium bubbles interact synergistically with the matrix hardening to decrease the ductility of the metal. Above 650°C, recrystallization begins and the defects anneal out. There is a slight increase in ductility in this region, due to the "softening" of the matrix, but above 700°C recrystallization becomes complete and the decrease in ductility is almost entirely due to helium embrittlement.

FIGURE VIII - REFERENCE 17

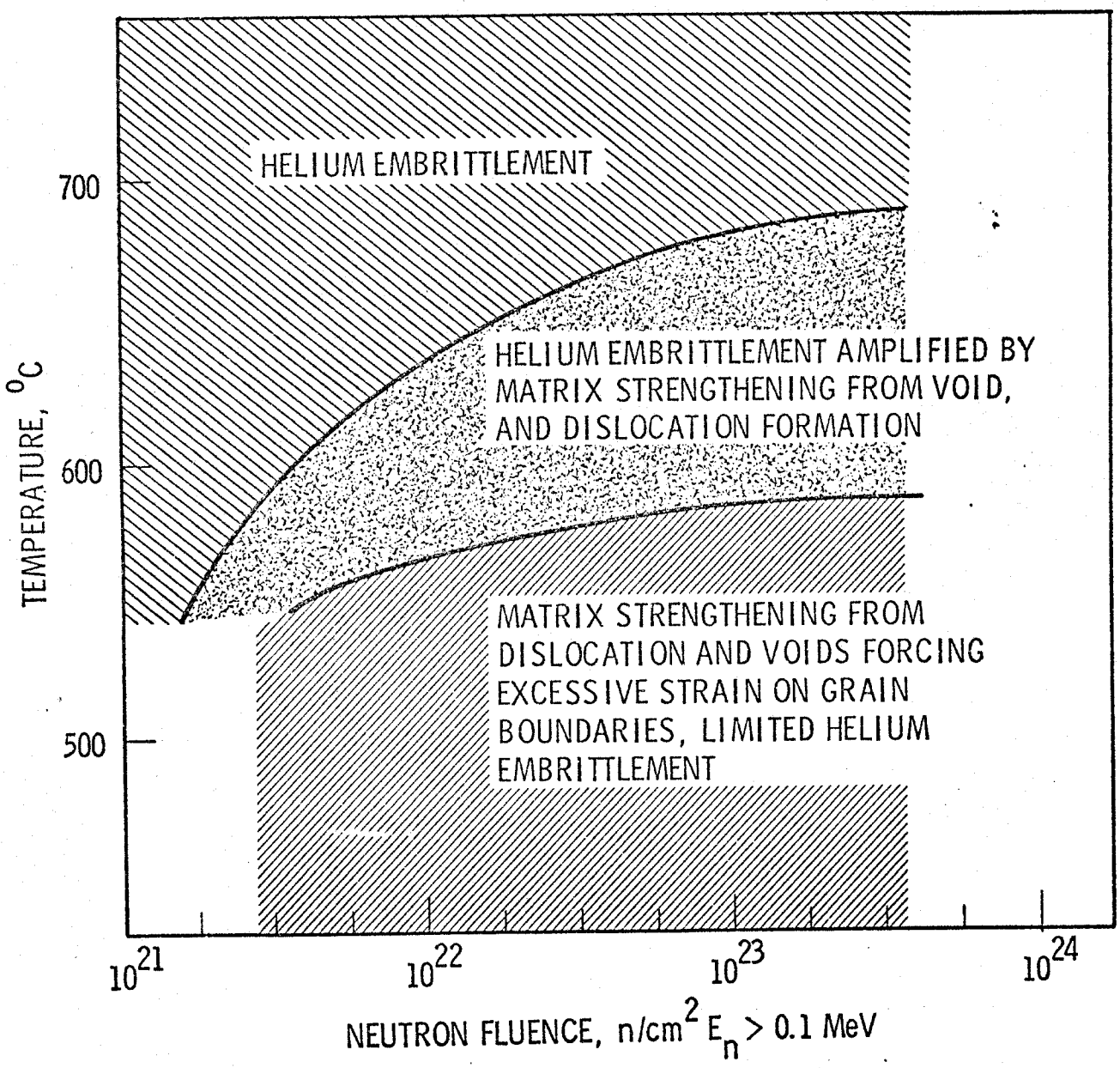

The type of embrittlement that occurs in stainless steel is a function of both temperature and fluence. The domains for each type of embrittlement are shown in Figure VIII. At temperatures below 540°C, matrix hardening predominates and at high temperatures, helium embrittlement predominates. The upper boundary of the intermediate region where the two phenomena amplify each other, is fluence dependent. This upper limit matrix hardening due to voids increases as fluence increases. The pre-irradiation heat treatment of the tensile specimens can also determine what effects irradiation has on ductility.[14,15,22,23] The initial ductility of cold worked specimens is much lower than annealed specimens. The matrix of a cold worked sample is strain hardened prior to irradiation and the effect of displacement damage is not as great in cold worked samples as it is in annealed samples. At high temperatures, where helium embrittlement predominates, the effect of heat treatment is not so great. These general trends have been observed by Ward et. al.[15] who irradiated specimens of annealed and 20% cold worked 316 stainless steel to fluences of 7×10^{21} nvt ($E > 0.1$ MeV) at a temperature of 1100°F (595°C) in EBR-II. The results of this experiment as a function of test temperature are shown in Figure IX. In all cases, the ductility of the annealed specimen is higher than the cold worked specimens. At higher fluences, the cold worked material will inhibit void formation which may allow it to exhibit higher ductility than the annealed material.

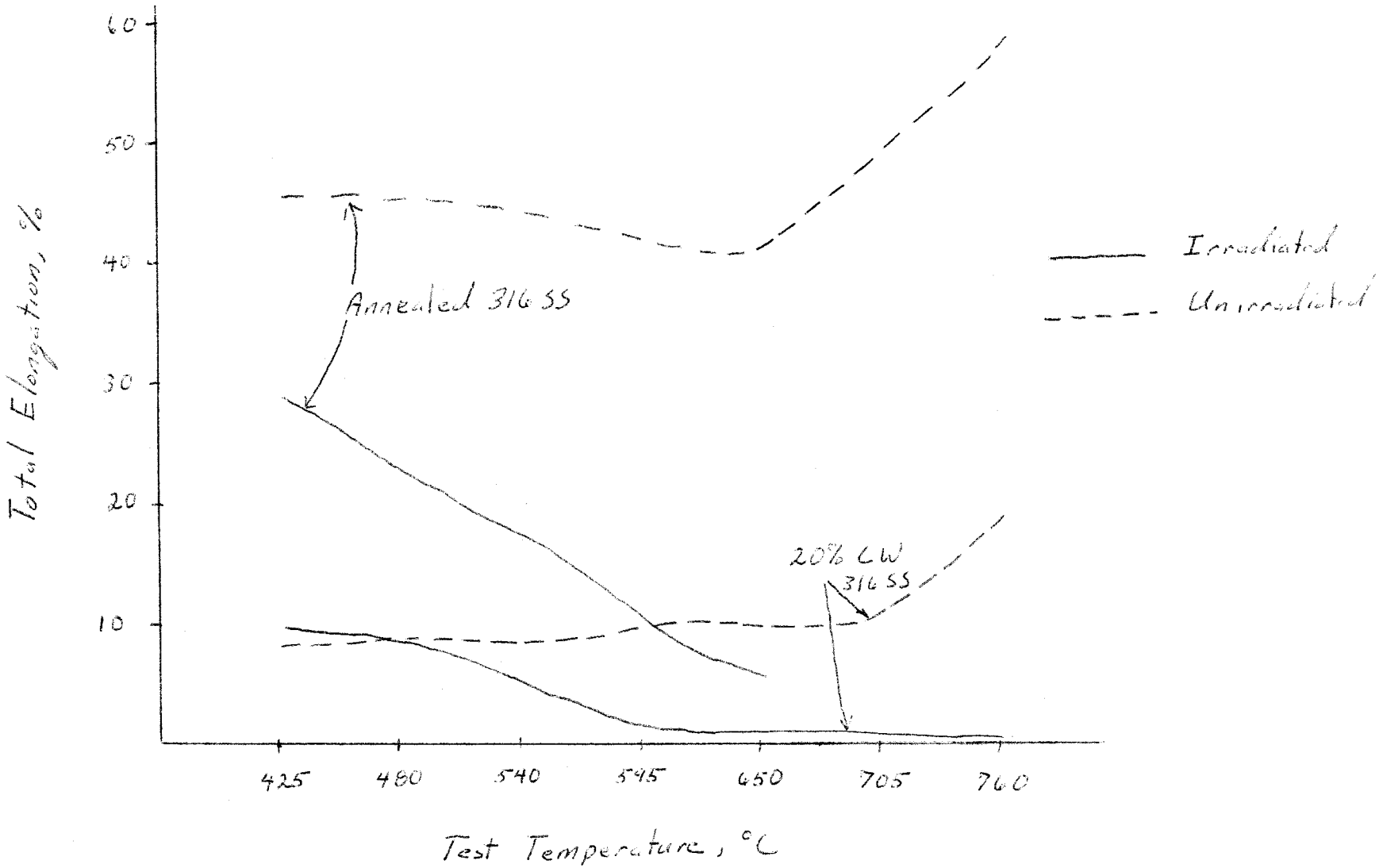

$\phi t = 7 \times 10^{21}$ n/cm²

Irradiation temperature 540°C

Figure IX

A.L. Ward, L.D. Blackburn, A.T. Lovell, Trans. Am. Nucl. Soc., 13 - Ref. 15

Embrittlement in the Wisconsin Fusion Reactor

The University of Wisconsin Controlled Thermonuclear Reactor (UWCTR)[16] provides a conservative design of a fusion reactor that can be used to make predictions about materials behavior. To alleviate the problems of radiation damage and lithium corrosion, the reactor is designed to operate at low wall loadings (0.53 MW/m^2) and low temperatures (<500°C). The structural components of this system are to be made of 316 stainless steel. The reduction in the ductility of these structural components will be a problem in fusion reactors, just as it will be in fast fission reactors.

The major difference between embrittlement in fast reactor fusion reactors is the neutron energy spectra. A predicted flux spectrum for the UWCTR has been developed[16] and discussed previously. Due to the high energy neutrons in the fusion reactor, the gas production rates are much higher than can be simulated in fast reactors.[1] In addition, the tritium in the lithium coolant may diffuse into the stainless steel and decay to helium-3 providing another important source of helium.[6] However, the displacement damage rate is much lower than the corresponding rate in a fusion reactor. This difference in flux spectrums makes the application of results from fast reactor irradiation to fusion reactors quite difficult.

For the purposes of this paper, helium embrittlement and embrittlement due to displacement damage will be considered separately. However, it must be realized that the fusion reactor may be operating in a temperature region where the two effects interact. This interaction

may decide the ductility limit and failure mode of the stainless steel.

The data developed by Holmes, Lovell and Fish[17] for annealed type 316 stainless steel irradiated in EBR-II will be used to make predictions about the effect of irradiation on the ductility within the UWCTR system. Because there are so many important variables, it is essential that one consistent set of data be used for any calculations. This set of data recently developed, spans a wide range of temperatures and extends to fluences approaching $10^{23} n/cm^2$. Unfortunately, EBR-II is not able to operate at temperatures below ~350°C while some parts of the UWCTR will be at temperatures down to 280°C. Hence, some of the data in the important low temperature region will be available. Annealed stainless steel was chosen because the data was more complete and the results seem to be more optimistic. The ductility is measured in terms of uniform elongation because it is felt that the onset of plastic instability will be an untenable situation.

The results of this study by Holmes et.al. are presented in Figure X. All of the irradiations were performed at the test temperature. At 430 and 480°C, the values of uniform elongation measured decrease sharply and are relatively independent of temperature. This behavior may be due to the onset of void formation. In order to compare the EBR-II fluence to UWCTR conditions, additional scales have been added to Figure X indicating the amount of helium produced and number of displacements per atom in the corresponding EBR-II fluence.

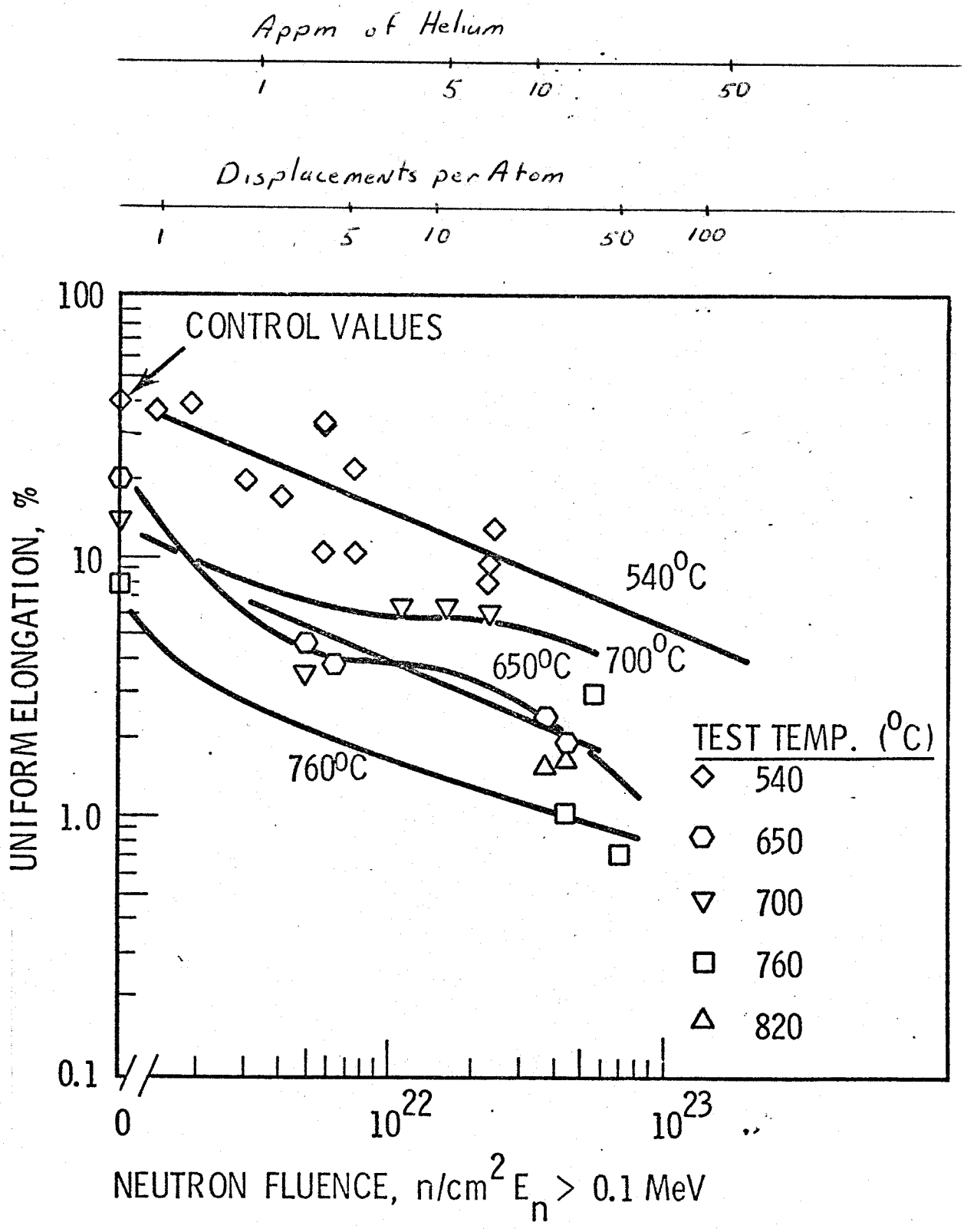

Figure X a.

Ref 17

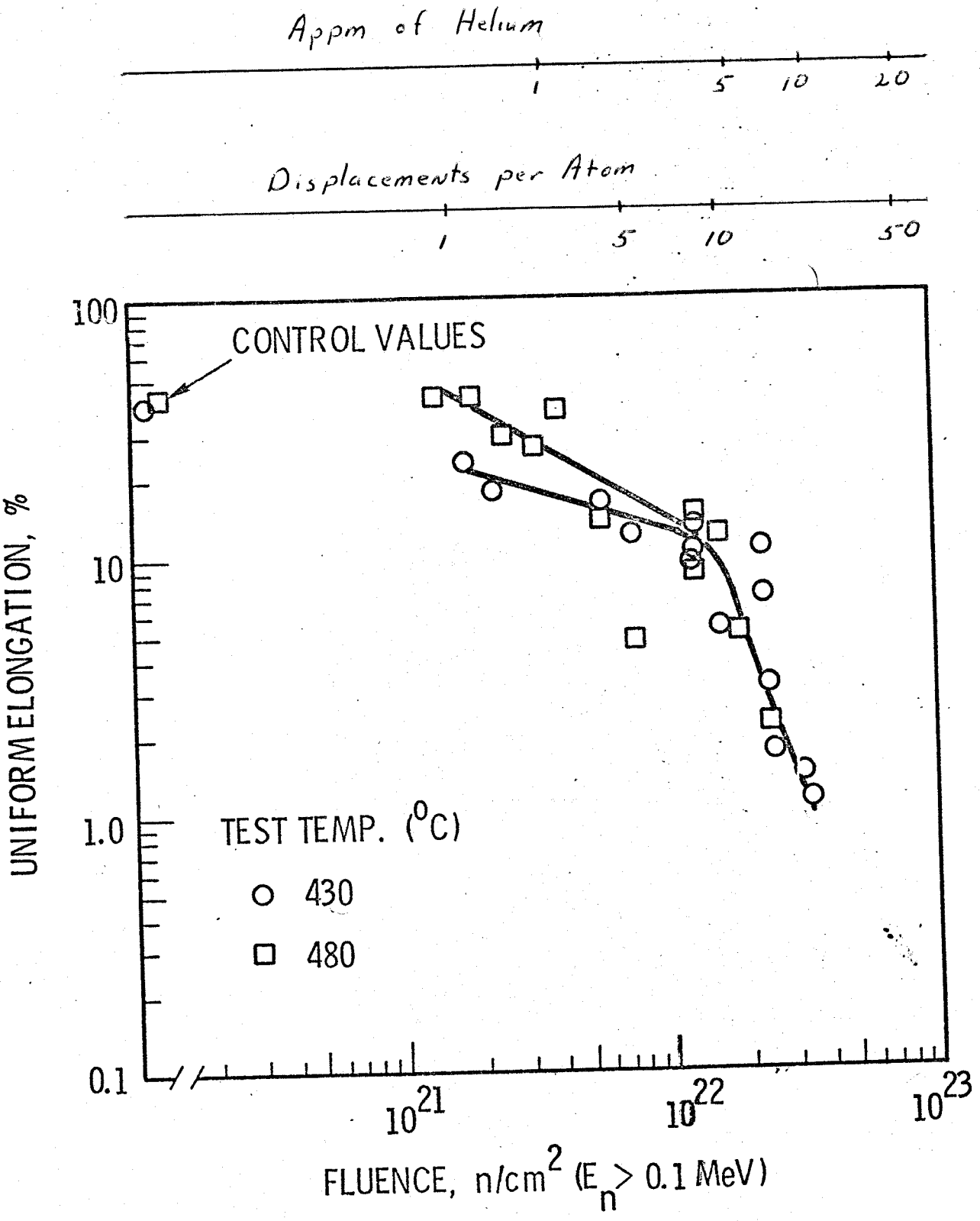
Appm of Helium
1
5
10
20
Displacements per Atom
1
5
10
50
100
10
1.0
0.1
CONTROL VALUES
TEST TEMP. (°C)
430
480
UNIFORM ELONGATION, %
10^{21}
10^{22}
10^{23}
FLUENCE, n/cm^2 (E_n > 0.1 MeV)

Figure X b

The helium production rates are based on a spectral averaged cross section of 25 millibarns measured in EBR-II by McElroy, Farrar and Knox.[18] The displacement values are based on the assumptions that $10^{22} n/m^2$ (E > 0.1 MeV) is equivalent to 7.03 dpa.

An arbitrary lower ductility limit of 1% (uniform elongation) has been assumed for the UWCTR. In the EBR-II irradiations, at a temperature of 480°C, this limit was reached at a total fluence of 3.6×10^{22} n/m^2 (E > 0.1 MeV). This limit corresponds to an ultimate tensile strength of 110,000 lbs/in^2.[13] A rough estimate of the amount of energy that this material can absorb, E_{abs}, can be found by assuming that it will fail in a brittle manner such that

$$E_{abs} = 1/2 \text{ (Uniform Elongation) (Ultimate Tensile Strength)}$$

$$= 0.5(0.1 \text{ in/in}) (110{,}000 \text{ lbs/in}^2)$$

$$= 550 \frac{\text{in-b}}{\text{in}^3}$$

$$= 3.79 \text{ Joules/cm}^3$$

The total volume of the first wall of the UWCTR is approximately 8.6×10^7 cubic centimeters. This limit of ductility then implies that under uniform loading, the first wall could absorb approximately 3.26×10^8 Joules. This is a rough calculation and provides an upper limit as it does not include the effects of stress concentration due to non-uniform loading or defects in the structure.

By assuming that all of the embrittlement in the EBR-II irradiated specimen was due to displacement damage, an estimate can be made for the time it will take to reach the 1% ductility limit on the UWCTR system.

The fluence limit of 3.6×10^{22} n/cm^2 corresponds to 34.8 displacements per atom. The displacement rate at several positions in the UWCTR system has been calculated by Kulcinski.[19] From this information, the time to reach the 1% ductility limit has been calculated as a function of position in the blanket. The results of these calculations are shown in Figure XI. The first wall will reach this limit in approximately two and one-half years. This means that the first wall will have to be replaced eight times in the twenty year life of the reactor. All of the material in the first 35 centimeters of the blanket will reach the 1% ductility limit within the design life of the plant.

Another limit may be calculated by assuming that the helium produced is solely responsible for the reduction in ductility. As noted previously, the EBR-II fluence values can be converted to helium concentrations by using a spectral averaged cross section. The limiting value of 3.6×10^{22} n/cm^2 corresponds to a concentration of 10.17 appm of helium. Helium production rates for various positions in the reactor have been reported in an earlier paper.[1] The time to reach this limiting helium concentration has been plotted as a function of distance from the first wall of the reactor has also been plotted in Figure XI. Helium is produced at a much faster rate in the fusion reactor than it is in EBR-II. The first wall of the UWCTR would reach this maximum helium concentration in less than one month. Within ten years, all of the material within 150 centimeters of the first wall

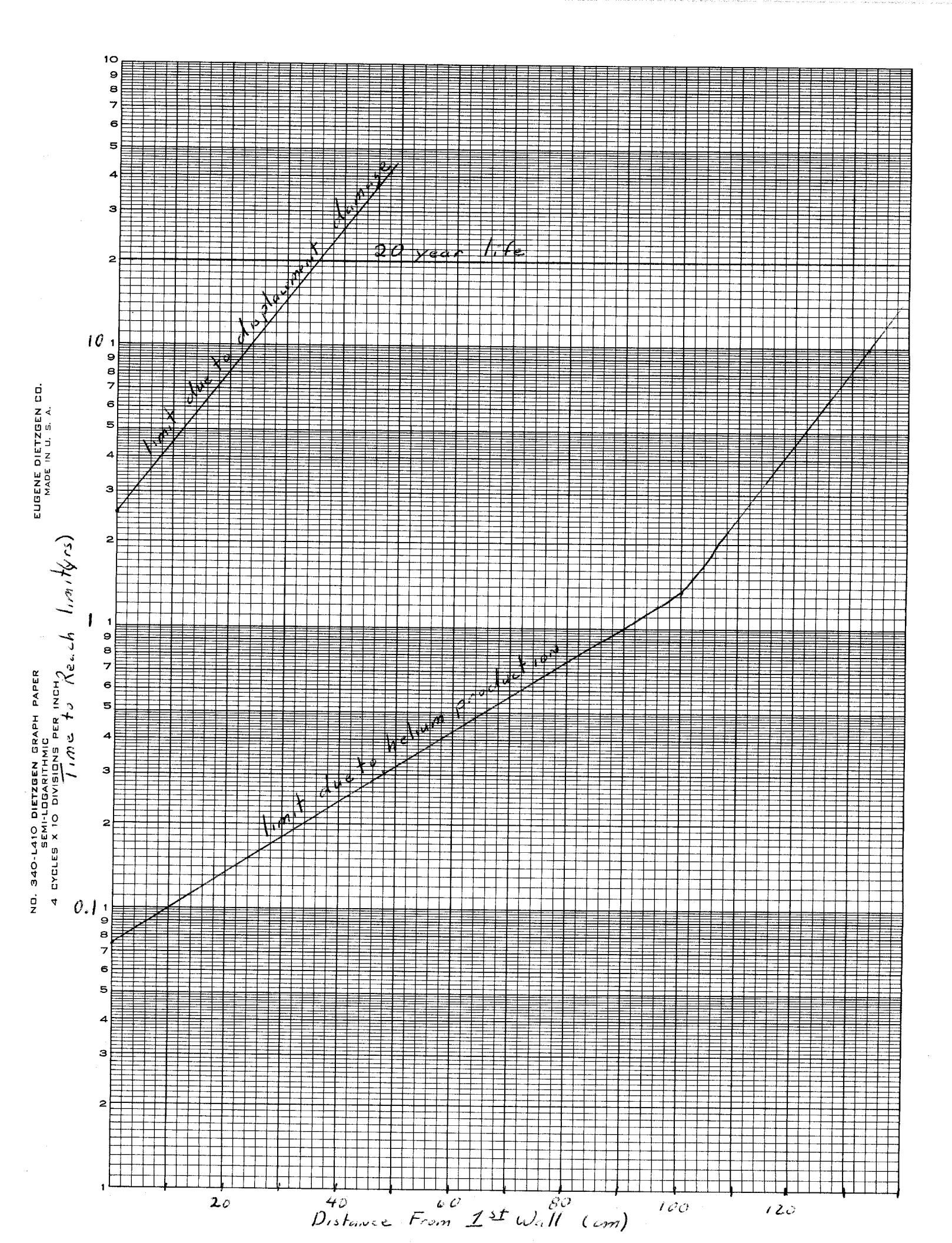

would reach this limit. These helium concentrations surpass all of the data now available. It is impossible to predict how the nucleation and growth of helium bubbles will be affected by these high concentrations. The entire UWCTR system is designed to operate at temperatures below the threshold for helium embrittlement. However, it is entirely possible that these high helium concentrations may lower the threshold for bubble formation and seriously impair the ductility of the material. However, the previously cited work of Kaglinanski et.al.[8] indicates that at low temperatures, the formation of helium bubbles on the grain boundaries does not decrease the ductility of the material. If the low temperature ductility is severely decreased by the formation of gas bubbles, temperature excursions and localized hot spots will not be tolerable in the system.

These results may be better understood by referring back to Figure VII, where ductility is plotted as a function of irradiation temperature. The first wall of the UWCTR operates at temperatures between 300 and 500°C. The upper part of this temperature range corresponds to the region just before bubble formation begins, where the ductility has increased due to a reduction in defect concentration. However, the low temperature part of the walls where large concentrations of small defects are produced, will undergo severe embrittlement due to matrix hardening. The exact effects in this lower temperature range are not known because EBR-II irradiation conditions are limited to higher temperatures.

Conclusions

The ductility of the structural material in a fusion reactor is going to be severaly reduced by irradiation. The rate of helium production in this system is so high that the reactor must be operated at temperatures where helium embrittlement is not important. This implies that the reactor must be operated at temperatures below 500°C. If the threshold for bubble formation is significantly reduced at these high helium concentrations, materials with lower gas production rates and higher resistance to helium embrittlement will have to be found. There is at this time only limited data for other materials.[6,25] However, if the embrittlement is due entirely to displacement damage, the loss of ductility in the UWCTR system will be comparable to the problems encountered in fast reactor technology. In order to predict the effects of irradiation on the UWCTR system, more data must be compiled for lower temperatures and higher helium concentrations.

REFERENCES

1. R. Lott, "Transmutation Effects in Nuclear Reactors," March 1973.

2. Ductility, ASM, Metal Park, Ohio, October 1967.

3. Irradiation Effects on Structural Alloys for Nuclear Reactor Applications, ASTM STR. No. 484, Niagara Falls, (June 29 - July 1, 1970).

4. D. Kramer, H. R. Brager, C. G. Rhodes and A. G. Pard, "Helium Embrittlement in Type 304 Stainless Steel," J. Nucl. Mat. 25, 121, (1968).

5. R. Brown, "Swelling of Fast Neutron Irradiated Austenitic Stainless Steel and Its Effect on the UWCTR Design," February 1973.

6. T. W. Scott, "Hydrogen Embrittlement and Other Effects in Thermonuclear Reactor Materials," to be published.

7. C. W. Hunter, R. L. Fish, J. J. Holmes, "Channel Fracture in Irradiated EBR-II Type 304 Stainless Steel," HEDL-SA-369 S, (1972).

8. M. Kangilaski, F. T. Zurey, J. S. Perrin and R. A. Wullaert, "Relationship of Microstructure to Embrittlement in Irradiated Stainless Steel at Elevated Temperatures," J. Nucl. Mat., 39, 117, (1971).

9. A. L. Ward and J. J. Holmes, "Ductility Loss in Fast Reactor Irradiated Stainless Steel," Nucl. App. & Tech., 9, 771, (1970).

10. D. A. Woodford, J. P. Smith and J. Moteff, "Observation of Helium Bubbles in an Irradiated and Annealed Austenitic Steel," J. of the Iron and Steel Inst., 70, (1969).

11. D. A. Woodford, J. P. Smith and J. Moteff, "Effect of Helium Gas Bubbles on the Creep Ductility of an Austenitic Alloy," J. Nucl. Mat., 29, 103, (1969).

12. E. E. Bloom and J. R. Weir, Jr., "Effect of Neutron Irradiation on the Ductility Loss of Austenitic Stainless Steel," Nucl. Tech 16, 45, (1972).

13. R. L. Fish and J. J. Holmes, "Tensile Properties of Annealed Type 316 Stainless Steel After EBR-II Irradiation," HEDL-SA-421, (1972).

14. J. S. Watkin, J. P. Shepherd, J. Standring, "Effects of Irradiation on the Tensile and Structural Properties of FV548 Stainless Steel," presented at ASTM Symposium, Effects of Irradiation on Structural Materials, Los Angeles, (June 1972).

15. A. L. Ward, L. D. Blackburn and A. J. Lovell, "Mechanical Properties of EBR-II Irradiated 20% Cold Worked Type 316 Stainless Steel," Trans. Am. Nucl. Soc., 13, 593, (1970).

16. M. A. Abdou et. al. "Preliminary Conceptual Design of a Tokamak Reactor," to be published in Proceedings of Texas Symposium on the Technology of Controlled Thermonuclear Fusion Experiments and the Engineering Aspects of Fusion Reactors.

17. J. J. Holmes, A. J. Lovell and R. L. Fish, "Ductility of Irradiated Type 316 Stainless Steel," HEDL-SA-310, (1972).

18. W. N. McElroy, H. Farrar IV and C. H. Knox, "Helium Production Cross Sections for Elements Irradiated in EBR-II," Trans. Am. Nucl. Soc., 13, 314, (1970).

19. G. L. Kulcinski, personal communication.

20. R. Sumerling and D. Rhodes, "Effect of Tensile Test Conditions on the Fracture Behavior of 20 Cr-25 Ni-Nb Stabilized Stainless Steel After High-Temperature Irradiation," J. Nucl. Mat., 40, 121, (1971).

21. H. J. Busbomm, C. F. Barrett, P. J. Ring, C. N. Spalaris, "Application of Postirradiation Ductility Data to Fuel Rod Failure LImits," Trans. Am. Nucl. Soc., 15, 738, (1972).

22. Ph. Van Asbroeck, M. Snykers, W. Vandermeulen, "High-Temperature Embrittlement of Ferritic and Austenitic Stainless Steels Irradiated up to 1.6 x 10^{22} n/cm^2 (>0.1 MeV)," presented at ASTM Symposium, Effects of Radiation on Structural Materials, Los Angeles, (June 1972).

23. R. L. Fish, A. J. Lovell, H. R. Brager and J. J. Holmes, "Tensile and Creep Behavior of Cold Worked Type 316 Stainless Steel After EBR-II Irradiation," HEDL-SA 468, (1972).

24. R. L. Fish, J. L. Straalsund, C. W. Hunter, J. J. Holmes, "Swelling and Tensile Property Evaluation of High Fluence EBR-II Thimbles," HEDL-SA 321, (1972).

25. T. T. Claudson, "Quarterly Progress Report Irradiation Effects on Reactor Structural Materials," HEDL-TME-77-144, (1972).

26. K. R. Garr, D. Kramer and C. G. Rhodes, "The Effect of Helium on the Stress Rupture Behavior of Type 316 Stainless Steel," Met. Trans., 2, 269, (1971).

27. D. Kramer, K. R. Garr, A. G. Pard and C. G. Rhodes, "A Survey of Helium Embrittlement of Various Alloy Types," AI-AEC-13047, (1972).